Supporting Information

Hollow Mesoporous Hydroxyapatite Nanoparticles (hmHANPs) with Enhanced Drug Loading and pH-Responsive Release Property for Intracellular Drug Delivery

Ya-Huei Yang,[a] Chia-Hung Liu,[b] Yung-He Liang,[a] Feng-Huei Lin[c,d] and Kevin C.-W. Wu*[a,c]

[a] *Department of Chemical Engineering, National Taiwan University, No. 1, Sec. 4, Roosevelt Road, Taipei 10617, Taiwan*

[b] Department of Urology, Taipei Medical University-Shuang Ho Hospital, No. 291, Jhongjheng Rd., Jhonghe Dist., New Taipei City 23561, Taiwan.

[c] *Division of Medical Engineering Research, National Health Research Institutes, 35 Keyan Road, Zhunan, Miaoli County 350, Taiwan*

[d] *Institute of Biomedical Engineering, National Taiwan University No. 1, Sec. 1, Jen-Ai Road, Jongjheng District, Taipei City 100, Taiwan*

***Corresponding Author's E-mail:** kevinwu@ntu.edu.tw

Experimental

Chemicals

Calcium acetate monohydrate, sodium bicarbonate, ethylene glycol, and acetic acid were obtained from J.T. Baker. MEM-Eagle, fetal bovine serum, sodium bicarbonate solution (7.5 %), L-Glutamine, penicillin, and 10X PBS were purchased from Level (Taiwan). Phosphoric acid, doxorubicin hydrochloride (DOX), hydrochloric acid (37 %), 4',6-diamidino-2-phenylindole (DAPI), 3-(4,5-dimethylthiazol-2-yl)-2,5-diphenyltetrazolium bromide (MTT), dimethyl sulfoxide (DMSO, 99.5 %), calcium D-gluconate ($[HOCH_2[CH(OH)]_4CO_2]_2Ca$), potassium hydrogen phosphate (K_2HPO_4), sodium hydroxide (NaOH), ethanol (C_2H_5OH, 95 %), and Pluronic F127 (poly(ethylene glycol)$_{106}$-poly(propylene glycol)$_{70}$-poly(ethylene glycol)$_{106}$) were all purchased from Sigma-Aldrich.

Synthesis of Hydroxyapatite Nanoparticles (HANP) and Hollow Mesoporous Hydroxyapatite Nanoparticles (hmHANP)

The HANPs without a hollow core and mesoporous shell structure were synthesized by modifying the method presented in a previous report (*Sci. Technol. Adv. Mater.*, 2011, **12**, 045005-045010.). Typically, F127 (3 g) and calcium D-gluconate (0.04 mol) were dissolved in distilled water (100 mL), and the mixture was stirred vigorously, until a clear sol solution was obtained. Potassium hydrogen phosphate (K_2HPO_4, 0.024 mol) dissolved in 60 mL distilled water was prepared, and its pH was adjusted to 12.0 using NaOH (2N). The PO_4^{3-} solution was then slowly added to the Ca^{2+}/F127 solution when stirring. A white precipitate formed after the entire mixture was heated at 90 °C for 24 h. The precipitate was then washed several times with boiling water and ethanol to remove excess calcium D-gluconate. The final product was then collected by filtration and dried at 100 °C for 24 h. The characterization of the synthesized HANP is shown in **Fig. S4 and S5**.

The HANPs with a hollow core and mesoporous shell structure were synthesized by modifying the method presented in a previous report (J. Mater. Chem., 2008, 18, 2722–2727), and the details were reported in our previous report (Curr. Nanosci., 2011, 7, 926-931). Hollow nanoparticles have been widely synthesized through selective etching of cores from the corresponding core/shell composites (so-called colloidal templating methods). Although the synthesis of hmHANPs was based on one such colloidal templating method, the reaction conditions for a successful hmHANP formation were systematically optimized (**Fig. S6-S10**). First, two 10 mL of ethylene glycol were separately added into a calcium acetic aqueous solution (0.3 M, 2 mL)

and a sodium bicarbonate aqueous solution (0.3 M, 2 mL). These two solutions were then mixed together. After reacting for 3 h, the mixed solution gradually became turbid, indicating the generation of calcium carbonate ($CaCO_3$) nanoparticles. A phosphoric acid solution (H_3PO_4, 0.01 M, 1 mL) was added to this solution, and the added phosphate ions replaced a number of carbonate ions to form a hydroxyapatite (HA) shell surrounding the $CaCO_3$ nanoparticles (referred as $CaCO_3$/HA core/shell composite). After reacting for 12 h, the core/shell composite was collected through centrifuge. To remove un-reacted reactants, the composite was washed with deionized water three times. Finally, the composite was immersed in an acetic acid solution (35 mM, 6.5 mL) to remove the CaCO3 cores, resulting in hollow hydroxyapatite nanoparticles with a mesoporous shell structure. The final hmHANP product was first washed with deionized water for two to three times to remove residual acetic acid, and then dried in a vacuum.

Characterization

The crystalline phases of $CaCO_3$ and hmHANP were analyzed with an X-ray diffractometer (Rigaku Ultima IV), with Cu $K_{\alpha 1}$ radiation (1.5406 Å) at 40 kV and 40 mA. The porous properties of the HANPs and hmHANPs were analyzed using nitrogen adsorption/desorption isotherms on a Micromeritics ASAP 2000 instrument. The pore size distribution curve was obtained from the desorption isotherm using the Barrett-Joyner-Halenda (BJH) method. The specific surface area was calculated using the Brumauer-Emmett-Teller (BET) method. The morphologies, particle sizes, and porous structures of the $CaCO_3$ nanoparticles, $CaCO_3$/hydroxyapatite core/shell composites, and hmHANPs were observed with FE-SEM (FEI Nova NanoSEM 230) and TEM (JEOL JEM 2100F). The phosphorus concentration in the solutions was determined using the molybdenum blue method.

Preparation of DOX-loaded hmHANP

The anticancer drug, doxorubicin (DOX), was first dissolved in an aqueous solution at the desired concentration (10^{-3}, 10^{-4}, and 10^{-5} M). To this $DOX_{(aq)}$ solution, hmHANP (10 mg) was added under constant stirring for 24 hr at room temperature in a dark environment. The purple DOX-loaded hmHANPs (DOX@hmHANP) were then collected by centrifugation. To reduce the physical adsorption of DOX on the surface of DOX@hmHANPs, the purple precipitate was washed with deionized water, and dried in a vacuum. The fluorescent property of DOX (λ_{ex} = 470 nm and λ_{em} = 565 nm) effectuated calculating the loaded capacity and release percentage of DOX by photoluminescence microscope (PL).

Cell culture

BT-20 human breast cancer cells (ATCC® Number: HTB-19™) were used in this study. They were cultured in flasks with the MEM medium supplemented with 10 % fetal bovine serum, 2 % sodium bicarbonate, 1 % L-Glutamine, and 1 % penicillin at 37 °C under a humidified atmosphere containing 5 % CO_2.

Cell viability

Cell viability was investigated using MTT assay. First, BT-20 cells were cultured in a 24-well culture plate at a density of 1×10^5 cells per well, and allowed to attach overnight. The cell-attached plate was then washed with PBS solution three times, and immersed in serum-free MEM medium (0.5 mL/well) containing different concentrations of nanoparticles or drug-loaded nanoparticles. After incubation for different periods, the nanoparticle-immersed plate was washed several times with PBS solution to remove the nanoparticle residue. The MTT stock solution (5 mg/mL) was then diluted 10 times with serum-free MEM medium and added to each well (0.5 mL/well). These cells were further incubated for 4 h to allow the yellow dye to transform into blue formazan crystals. The un-reacted dye was then removed by aspiration, and DMSO (400 μL) was added to each well to dissolve the blue formazan crystals. Finally, the dissolved DMSO solution was transferred to a 96-well culture plate (100 μL/well), and its optical density was measured with an Elisa Reader at a wavelength of 570 nm.

Confocal Microscopy

BT-20 cells were seeded at a density of 1×10^5 cells per well in a 4-well culture plate with Lab-Tek chambered coverglasses at the bottom of each well. After incubation overnight, the BT-20 cells attached to the plate, and the MEM medium was replaced with different concentrations of drug-loaded nanoparticles in serum-free MEM medium (0.5 mL/well). The cell-plated coverglasses were then washed with PBS solution three times. A DAPI PBS buffer (2.80E-5 M, 1 mL) was then added to stain the cell nuclei for 30-60 minutes. After being washed with PBS solution, DAPI-stained coverglasses were examined to check the cellular localization of particles using a confocal fluorescence microscopy system (Leica TCS SP5 II) with a 63x oil immersion objective lens.

Measurement of phosphorus concentration by the molybdenum blue method

10 mg of hmHANP was mixed with acetate buffer solutions (10 mM, 4

mL, pH 4.5 or 7.4). After stirring for 1 hr at 37 °C, the solution was centrifuged. 0.8 mL of the supernatant was taken out and diluted to 50 mL before 8 mL of the molybdenum solution was added. After reaction for 10 mins, the absorption at 880 nm was read to determine the concentration of the phosphorus. The calibration curve was done using KH_2PO_4 as a reference.

Calculation for loading and release of drug

- Loading capacity (mol/g) = mole of drug loaded divided by gram of nanovehicles (HANP or hmHANP).

(The loading capacity (mg/g) = $543.52 \times 10^3 \times$ loading capacity (mol/g)).

- Loading efficacy (%) = loading capacity divided by maximum loading capacity × 100.

(The maximum loading capacity was determined by adding the same amount of hmHANPs into a series of DOX solutions with different concentrations.)

- Release amount (mole/g) = mole of drug released from nanovehicles divided by gram of drug loaded nanovehicles.
- Release percentage (%) = release amount divided by loading capacity × 100.

Results & Discussion

Characterization of the synthesized hmHANP

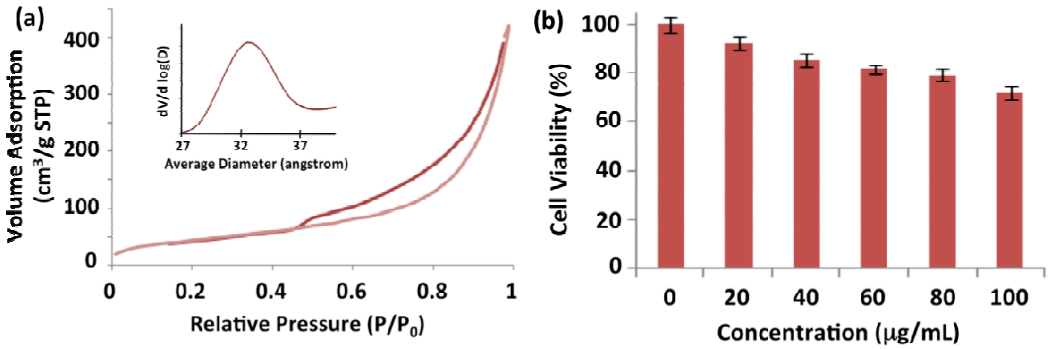

Figure S1. (a) Nitrogen adsorption/desorption isotherm and pore size distribution (inset) for hmHANP. (b) MTT assays of BT-20 cells treated with various concentrations of hmHANP.

The difference between release percentages of DOX from DOX@hmHANPs released at two different pH values

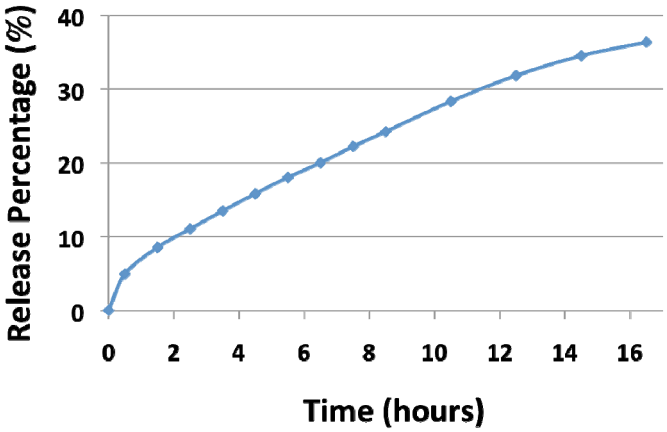

Figure S2. A linear relation between time and release percentage that was obtained from subtraction of release amount at pH 7.4 from that at pH 4.5.

MTT assays of BT-20 cells treated with DOX@hmHANPs (100 μg/mL) for different time

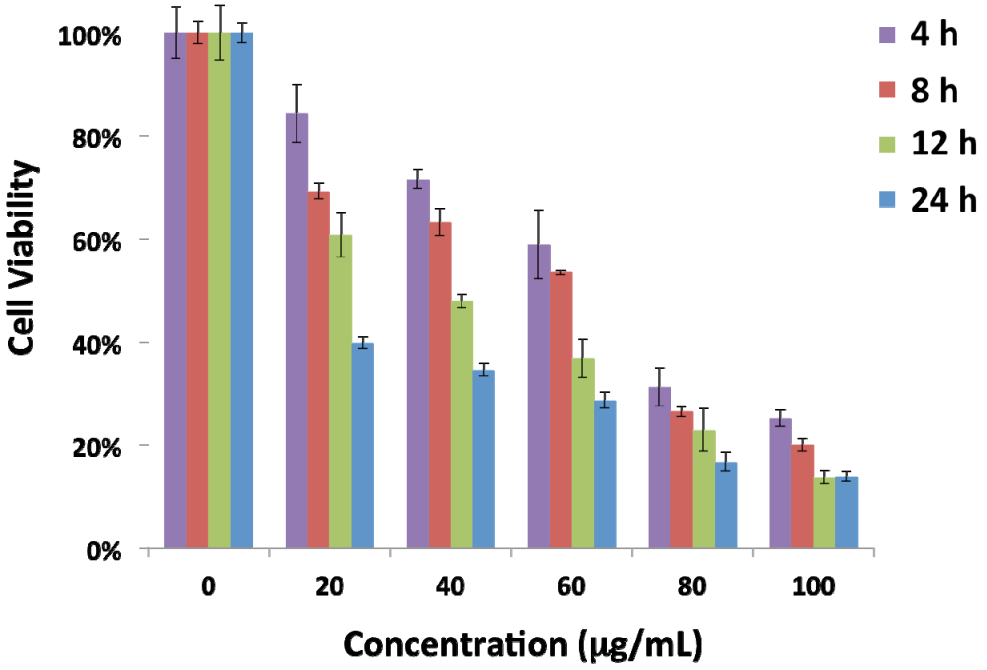

Figure S3. MTT assays of BT-20 cells treated with DOX@hmHANPs (100 μg/mL) for different time.

Characterization of synthesized HANP

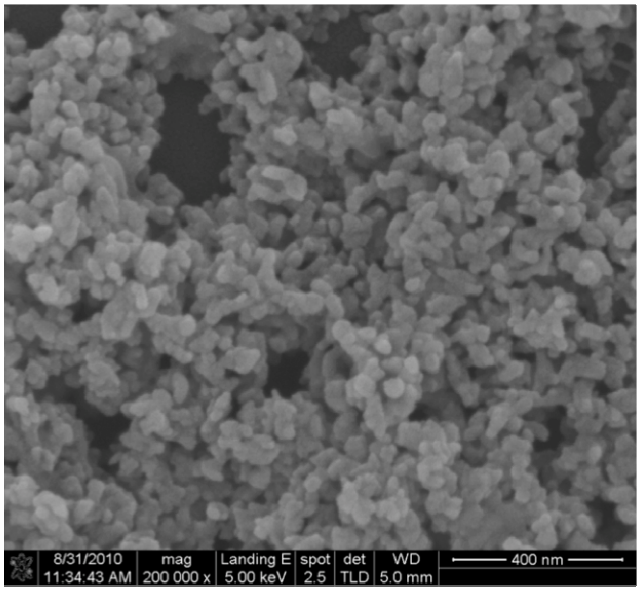

Figure S4. A typical SEM image of HANPs synthesized in this study.

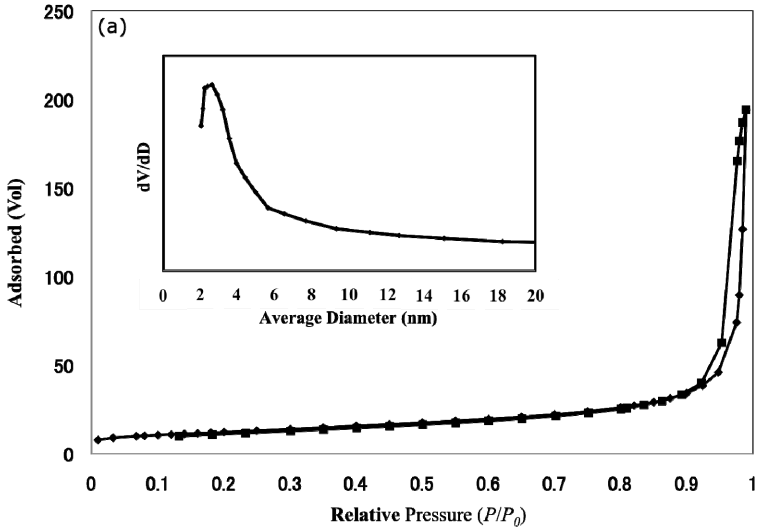

Figure S5. A nitrogen adsorption/desorption isotherm and pore size distribution (inset) of HANPs synthesized in this study.

Optimization of synthetic conditions for hmHANP

1. Effect of the amount of ethylene glycol (EG). The optimal ratio is 1:5.

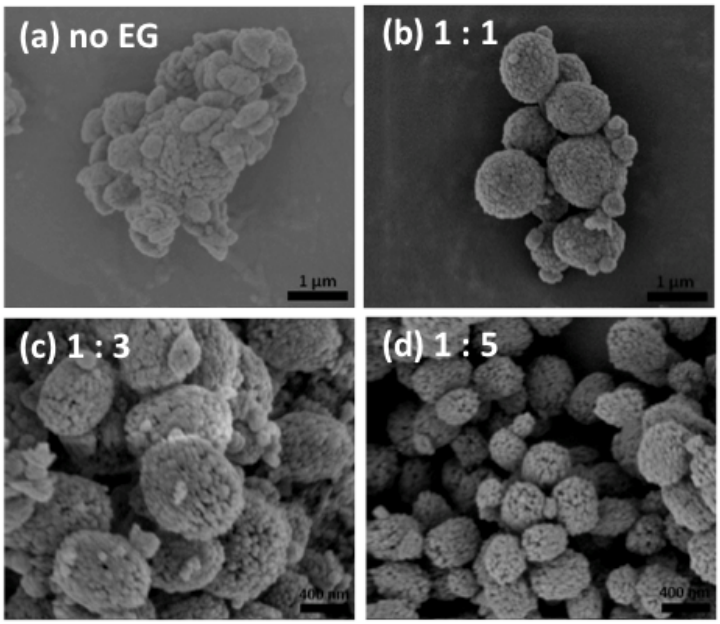

Figure S6. SEM images of $CaCO_3$ nanoparticles synthesized at different ratios of $CaCO_3$ precursor solution to EG.

2. Effect of the concentrations of $Ca(CH_3COO)_{2(aq)}$ and $NaHCO_{3(aq)}$. The optimal ratio is 0.3 M: 0.3 M.

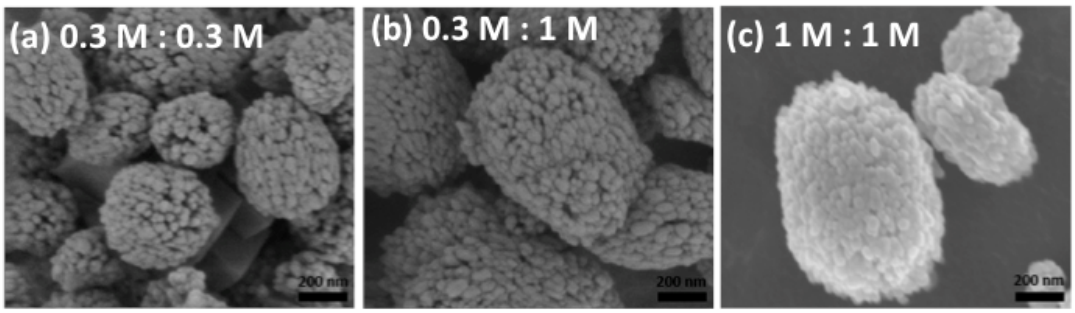

Figure S7. SEM images of $CaCO_3$ nanoparticles synthesized at different ratios of $Ca(CH_3COO)_{2(aq)}$ to $NaHCO_{3(aq)}$.

3. Effect of reaction time for formation of $CaCO_3$ nanoparticles. The optimal time is 3 h.

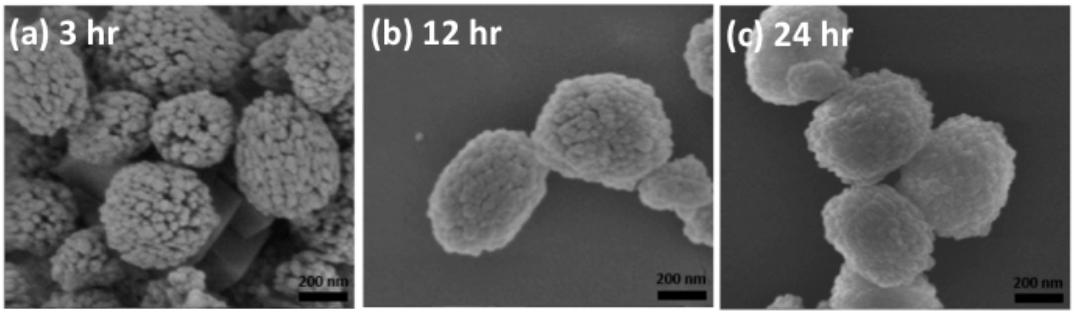

Figure S8. SEM images of $CaCO_3$ nanoparticles synthesized at different reaction time.

4. Effect of concentrations of $H_3PO_{4(aq)}$ for formation of $CaCO_3$/hydroxyapatite core/shell structure. The optimal concentration of $H_3PO_{4(aq)}$ is 0.01 M.

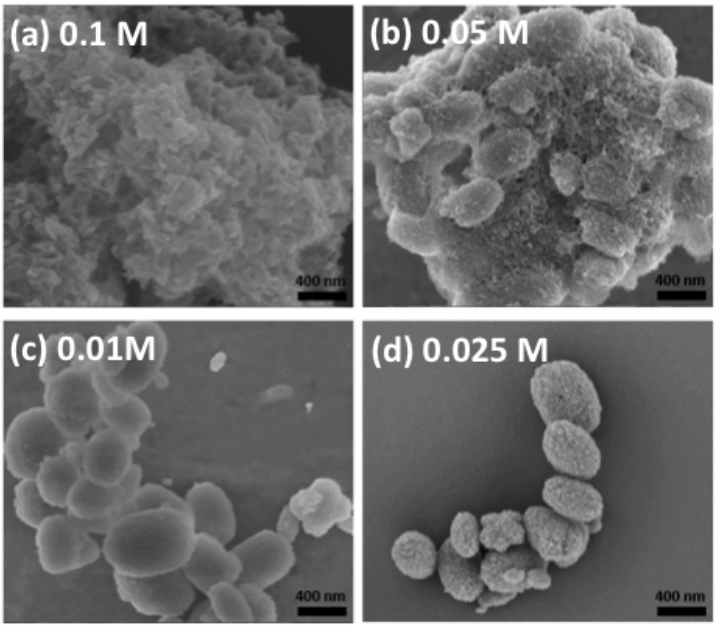

Figure S9. SEM images of $CaCO_3$/hydroxyapatite core/shell structure synthesized at different concentrations of $H_3PO_{4(aq)}$

5. Effect of the amount of $CH_3COOH_{(aq)}$. The optimal ratio of $CaCO_3$ precursor solution to $CH_3COOH_{(aq)}$is 1:3.125.

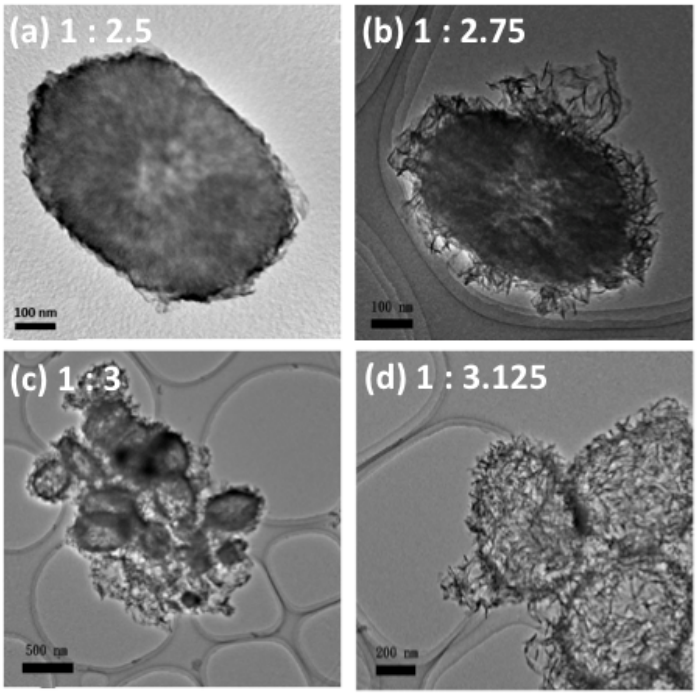

Figure S10. TEM images of $CaCO_3$/hydroxyapatite core/shell structures after washing by $CH_3COOH_{(aq)}$ with different ratios of $CaCO_3$ precursor solution to $CH_3COOH_{(aq)}$.